PROCEEDINGS : CAMME-1996
©NML JAMSHEDPUR; pp170-190

Creep life prediction of single crystal superalloys

R.N. GHOSH

National Metallurgical Laboratory, Jamshedpur - 831 007, India.

ABSTRACT

There has been a limited attempt to map the creep performacne of superalloy single crystals for all possible orientations as it requires a very large number of experiments, some of which may run for several years. Conventional life prediction techniques would indeed require a large data-base for a reliable estimation of the creep life of a single crystal. Moreover single crystals with a tensile axis having a low symmetry orientation would undergo a time dependent rotation well. Therefore life prediction in this case is no doubt more complex and it needs an entirely different approach. Creep in single crystals is known to take place through viscous glides on several slip systems such as {111} <101>, {001}<110> and {111} {112> in the case of Ni based superalloys. The paper reviews he such information has recently led to the development of a generalised model of creep deformation in cubic single crystals. Using this approach it is possible to numerically simulate the creep test on a crystal of arbitrary orientation based on the material constants estimated from a limited database on <001> and <111> crystals. Although this approach has been used to explain the creep behaviour of SRR99 a Ni base superalloy it is applicable to any cubic crystal. Such an analysis not only helps to identify the operative slip systems but also predicts both strain-time plots and crystal rotations that are consistent with the experimental observations.

INTRODUCTION

Single crystal superalloys are now being used in critical components of modern aero-gas-turbines primarily because of their superior capabilities to withstand higher service temperature. In comparison to the conventionally cast and directionally solidified alloys such as Mar 002, Mar M200, single crystal superalloys viz. CMSX2, PWA 1480 and SRR99 offer an advantage of 50°C [1]. The performance of these alloys

however is a strong function of orientation.

As far as applications are concerned <001> is the most perferred orientation because it provides the best combination of creep and thermal fatigue resistance although <111> is likely to exhibit the best creep properties [2,4].

There has been a limited attempt to map the performance of superalloy single crystals for all possible orientations. Conventional life prediction techniques such as θ projection or Graham Walles method which have been used to model the creep resistance of conventional superalloys are purely empirical in nature. Both of these methods assume specific functional forms to represent the creep strain-time plot. These are given below :

Graham Walles : $\varepsilon = at^{1/3} + bt + ct^3$ ... 1

Theta projection : $\varepsilon = \theta_1 (1-\exp/(-\theta_4 t)) + \theta_2 (\exp(\theta_4 t)-1)$ ... 2

The constants a,b,c, θ_1, θ_2, θ_3 and θ_4 are functions of stress and temperature. Therefore it is imperative that a large volume of experimental database will be necessary for a complete characterisation of the above constants so that reliable predictions could be made for any arbitrary stress temperature conditions.

Orientation is an additional factor that is likely to influence the creep behaviour of such crystals. In cases where the loading axis does not concide with a symmetric crystallographic direction such as <001>, <011> or <111> the crystal is likely to undergo a time dependent rotation. This will subsequently affect the creep behaviour of the material. Thus an appropriate model for creep life prediction of a single crystal superalloy will be one which could predict not only creep strain time plot but also the time dependent rotation.

Extension of the conventional techniques to model the orientation dependence of creep of single crystal superalloys will be extremely difficult if not impossible. Besides it would require enormously large volume of experimental database on crystals having different initial orientations. This no doubt will be quite expensive and it would take a very long time to collect such information.

This has been the main impetus for the recent development of a predictive model based on the physics of creep deformation of single

crystals. This is based on the fact that the creep in these alloys takes place through viscous glides on certain slip systems such as {111}<101>, {111}<112> and/or {001}<110> in the case of Ni base super-alloys [5,6]. The purpose of the present paper is to examine the current status of such development and illustrate the advantage of physics based modelling over empirical approaches so far being used for creep life prediction.

PHYSICAL MODEL

Isotropic Model

The creep of single crystal superalloys like that of the equiaxed wrought and cast version is dominated by a progressively increasing strain rate over most of the creep life. This type of dominant tertiary creep behaviour in these alloys have been shown to be a result of strain softening due to the accumulation of mobile dislocations. There could be two variations of such softening depending on either linear or exponential accumulation of damage with creep strain. Dislocation creep models giving a quantitative description of such softening have been developed elsewhere in details [7-9]. This approach is based on the assumption that the material is isotropic. It is worth while to look at this before its extension to anisotropic material. Unlike pure metals most engineering materials have a very high yield stress because of additional strengthening mechanisms (such as solution or particle strengthening) that inhibit glide. It is believed that at the initial stages of the creep life the density of mobile dislocation (ρ) is low and with subsequent deformation it increases resulting in increasing strain rate. Thus the associated structural damage defined in terms of ρ could be represented by a dimensionless parameter ω; for example in the case of linear strain softening model

$$\omega = \frac{\rho - \rho_i}{\rho} \qquad \ldots \quad 3$$

where ρ_i is the initial dislocation density and its increment is given by $d\rho = \beta\rho_i \, d\epsilon$ where β is a constant. Since strain rate is determined by the Orowan equation

$$\epsilon = \rho b v \qquad \ldots \quad 4$$

where b is the Burgers vector and v is the dislocation velocity, it is possible to show that creep in such an alloy could be described by the following set of coupled equations.

$$\varepsilon = \varepsilon_i (1 + \omega_1)$$

$$\omega_1 = \beta_1^{\epsilon} \qquad \ldots \quad 5$$

Exponential strain softening on the other hand considers that the change of ρ is proportional to its current value. Thus

$$\rho = \rho_i \exp(\beta \varepsilon) \qquad \ldots \quad 6$$

If the damage parameter ω were defined as

$$\omega_2 = \ln (\rho/\rho_i) \qquad \ldots \quad 7$$

here as well the process of creep deformation could be analysed by a similar set of coupled differential equations given below

$$\varepsilon = \varepsilon_i \exp (\varepsilon_2)$$

$$\omega_2 = \beta_2 \varepsilon \qquad \ldots \quad 8$$

There could be cases where both the above mechanisms may occur in parallel. It has been shown by several workers that even though the intrinsic softening mechanism in Ni base superalloys is linear in nature but there can be an exponential softening component particularly when the test is performed under constant load condition. In such cases it is necessary to define two types of damages viz. ω_1 and ω_2 and their evolution law could be expressed by the following set of coupled equations

$$\varepsilon = \varepsilon_i (1 + \omega_2) \exp (\omega_2)$$

$$\omega_1 = \beta_1 \varepsilon$$

$$\omega_2 = \beta_2 \varepsilon \qquad \ldots \quad 9$$

Thus the ε - t plots of most isotropic superalloys could be analysed based on the model parameters ε_i, β_1 and β_2. ε here represents tensile strain. Therefore extending the above concept to model anisotropic behaviour of single crystal it is necessary to examine how tensile strain can be computed from the shear displacement components.

Crystallographic Anisotropy

Plastic deformation in a crystal by glide results in simple shear. This has a strain and a rotation component. Therefore when a crystal of an arbitrary orientation is subjected to uniaxial deformation, as in a

creep test its orientation is likely to change. However the indices of the slip system with respect to the crystallographic axes still remains the same. Hence it is convenient to represent the component of deformation with respect to the crystallographic axes as the main frame of reference. Let γ^k be the magnitude of shear strain on the k^{th} slip system (n^k_1 n^k_2 n^k_3) [b^k_1 b^k_2 b^k_3] (Fig. 1) where n^k_i, b^k_i represent the direction cosines of the slip plane normal and the slip direction respectively as given in Table 1.

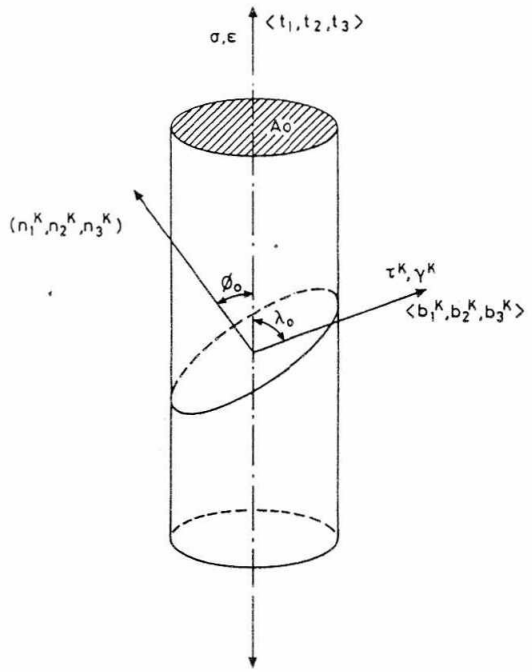

Fig. 1 : Schematic illustration showing the orientation of the slip plan and slip direction with respect to the tensile axis

***Table 1**:Direction cosines of the slip plane normal and slip direction with respect to the crystal axes*

OLD AXIS	NEW AXES		
	<100>	<010>	<001>
Slip direction	b^k_1	b^k_2	b^k_3
Slip plane	n^k_1	n^k_2	n^k_3

Ni base superalloy has a cubic crystal structure, hence the axes are rectangular. The approach described will be directly applicable to any cubic crystal. However if necessary it can be easily modified to suit any other types of crystals.

Physically γ^k represents the magnitude of the shear displacement along the slip direction $<b^k_1\ b^k_2\ b^k_3>$ on the slip plane $\{n^k_1\ n^k_2\ n^k_3\}$ In terms of the conventional axes systems this could be represented in the following form

$$\begin{bmatrix} 0 & \gamma^k & 0 \\ 0 & 0 & 0 \\ 0 & 0 & 0 \end{bmatrix} \qquad \ldots\ 10$$

which can be easily transformed into the crystallographic frame of reference following the transformation rule for rectangular axes system. Thus in this new frame of reference the components of displacement gradient can be represented as follows : (10)

$$\gamma^k \begin{bmatrix} b^k_1 n^k_1 & b^k_1 n^k_2 & b^k_1 n^k_3 \\ b^k_2 n^k_1 & b^k_2 n^k_2 & b^k_2 n^k_3 \\ b^k_3 n^k_1 & b^k_3 n^k_2 & b^k_3 n^k_3 \end{bmatrix} \qquad \ldots\ 11$$

When such a displancement takes place in a crystal through glide on several slip systems, the resultant component of the total displacement gradient e_{ij} can be obtained from the summation

$$e_{ij} = \sum_{k=1}^{N} \gamma^k \ b^k_i \ n^k_j \qquad \ldots\ 12$$

As a result of such small deformations on several slip systems the original tensile axis represented by the vector $[t_1\ t_2\ t_3]$ would change to $[T_1\ T_2\ T_3]$, a new vector representing the present tensile axis. Using matrix notation this transformation could be represented as

$$\begin{bmatrix} T_1 \\ T_2 \\ T_3 \end{bmatrix} = \begin{bmatrix} 1+e_{11} & e_{12} & e_{13} \\ e_{21} & 1+e_{22} & e_{23} \\ e_{31} & e_{32} & 1+e_{33} \end{bmatrix} \begin{bmatrix} t_1 \\ t_2 \\ t_3 \end{bmatrix} \qquad \ldots\ 13$$

The transformation matrix in the above equation is known as the deformation gradient matrix. This defines completely both the change in length and orientation of the crystal. For example, the axial strain ϵ can be obtained from the difference in the magnitude of the vectors representing the tensile axis before and after the deformation.

$$\epsilon = \frac{\overline{T} - \overline{t}}{\overline{t}} \qquad \ldots 14$$

A symmetric deformation gradient matrix would lead to no change in the orientation of tensile axis with respect to the cubic crystal axes (i.e., zero rotation) but does lead to a change in magnitude of the orientation vector. This condition occurs when the tensile axis coincides with a crystal axis of high symmetry such as [001], [011] or [111]. However, for crystals stressed in an arbitrary orientation, defined within the stereographic triangle by the angular coordinates (ϕ, ψ) defined in Fig. 2, the deformation gradient matrix will be assymetrical leading to both rotation and elongation. Thus the appropriate matrix representing tensile creep deformation of single crystal could be built if γ^k for specific slip systems were known.

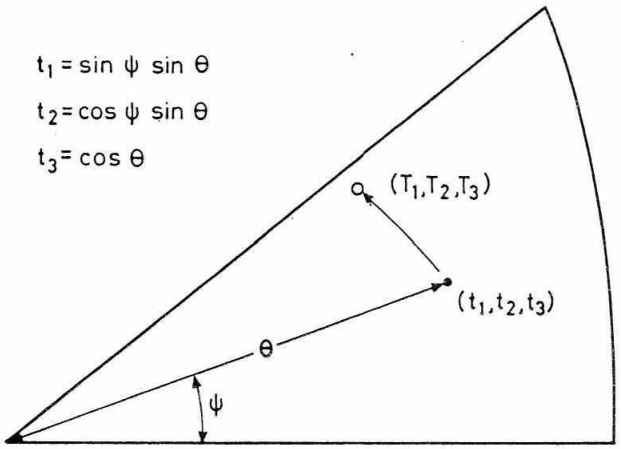

Fig. 2 : Schematic illustration showing angular relationship (ϕ, ψ) of the tensile axes before and after deformation with respect to crystallographic axes

It has been shown that in superalloys where creep is dominated by a linear softening mechanism, the process of deformation can be represented by a set of coupled differential equations describing the shear

strain rate and damage accumulation rate (ω^k) on a specific slip system [6].

$$\gamma^k = \gamma_i^k \left(1 + \omega_1^k\right)$$

$$\omega_1^k = \beta_1^k \, \gamma^k \qquad \ldots 15$$

Similar approach can also be used to show that in cases where exponential softening is the dominant mechanism of creep deformation γ^k and ω^k be given by

$$\gamma^k = \gamma_i^k \exp \omega_2^k$$

$$\omega_2^k = \beta_2^k \, \gamma^k \qquad \ldots 16$$

In single crystal superalloys there could be cases where both linear and exponential softening mechanisms may occur in parallel. The creep deformation process in such cases can be represented by a similar set of coupled differential equations

$$\gamma^k = \gamma_i^k \exp\left(\omega_1^k\right)\left(1 + \omega_2^k\right)$$
$$\omega_1^k = \beta_1^k \, \gamma^k$$
$$\omega_2^k = \beta_2^k \, \gamma^k \qquad \ldots 17$$

Depending on the appropriate mechanism of softening any ones of the equation sets (15-17), along with equations (12, 13) can be used to simulate the creep test on a crystal of arbitrary orientation on the basis of the model parameters γ^k_i and β^k. In order to interpolate or extrapolate from database it is necessary to describe the model parameters as function of stress and temperature after the exact mechanism of deformation has been identified. This approach has been used by Ghosh *et.al.*,[6] for a detailed analysis of the creep of SRR99, a Ni base single crystal superalloy. It is worthwhile to re-examine this in as it can be extended even to cases where different mechanisms operate.

DATA ANALYSIS

Recently Maldini and Lupinc have suggested that linear strain softening model is more applicable to Ni base single crystal superalloys [11]. This concluision is also supported by Curtis *et.al.*, from an analysis of an extensive database for SRR99 [12]. This analysis has shown that in the tensile formulation of creep deformation the initial characteristic creep rates ε_i were represented by an exponential function of stress. Adopting a parallel formulation the shear creep rates could be taken as

$$\dot{\gamma}_i^k = a_1^k \exp\left[a_2^k \tau^k - \frac{Q_1^K}{RT}\right] \qquad \ldots 18$$

where a^k_1 a^k_2 and Q^k_1 are constants and R is the universal gas constant and τ^k is the resolved shear stress on the k^{th} slip system.

Following Curtis et. al., the softening coefficient β^k can be described by a parallel procedure as for tensile formulation [12]. At low stresses β^k has a constant value that is independent of stress and temperature; at higher stresses β^k is described by

$$\beta^k = a_3^k \exp\left[\frac{Q_2}{RT} - a_4^k \tau^k\right] \qquad \ldots 19$$

Where a^k_3 a^k_4 and Q^k_2 are constants. At a given temperature and stress the minimum value of β^k given by the two algorithms is applicable.

Ghosh *et.al.*,[5] have shown that these constants can be estimated by converting their counterparts in tensile formulation through a geometrical factor which can be obtained either from eqn. (13) or from the Schimds' factor provided the slip system on which deformation takes place is known. Table 2 gives the Schimds' Factor and possible number of corresponding equivalent slip systems in face centered cubic lattice. Table 3 gives geometrical factors required to convert the tensile strain along a specific direction to the corresponding shear strain on a specific slip system.

Table - 2 : Schmid factors and the number of possible slip system {111} <101>, {111} <112> and {001} <110> slip associated with <001>, <011> and <111> oriented crystals.

	(111) <101>		(111) <112>		(001) <110>	
Tensile Axis	No.of Slip Systems	SF	No.of Slip Systems	SF	No.of Slip Systems	SF
<001>	8	0.4082	4	0.4714	6	0.0000
	4	0.0000	8	0.2357		
<011>	4	0.4082	2	0.4714	4	0.3536
	8	0.0000	4	0.2357	2	0.0000
			6	0.0000		
<111>	6	0.2722	3	0.3143	3	0.4714
	6	0.0000	6	0.1571	3	0.0000
			3	0.0000		

Table - 3 : Geometrical factors for converting tensile strain into shear strains along different slip directions

	Shear Strain (γ)		
Tensile Strain (ε)	(111) <101>	(111) <112>	(001) <110>
<001>	$8/\sqrt{6}$	$8/3\sqrt{2}$	0
<011>	$4/\sqrt{6}$	$4/3\sqrt{2}$	$\sqrt{2}$
<111>	$4/\sqrt{6}$	$4/3\sqrt{2}$	$\sqrt{2}$

It has been argued that in SRR99 or in Ni base superalloys in general slip could take place on the octahedral or the cubic slip system during creep. If tensile axis were along <001> then the resolved shear stress on the cube slip system will be zero (Table 2). Therefore in such cases the contribution towards creep strain will be entirely due to slip on the octahedral slip system. This formed the basis of converting the material constants a_1, a_2, a_3 etc., obtained from a detailed analysis of a fairly large database on the tensile creep of <001> crystals of SRR99, to the corresponding constants for octahedral slip in these alloys. These are given in the Table 4.

Table - 4 : Material constants for creep SRR99 in tensile and shear formulations

Parameters	Tensile Formulation for		Shear Formulation for		Unit
	<001>	<111>	(111) <101>	(001) <110>	
a^k_1	9.3×10^{13}	2.53×10^{-5}	2.85×10^{13}	1.79×10^{-5}	S^{-1}
a^k_2	1.77×10^{-2}	5.57×10^{-3}	4.34×10^{-2}	1.18×10^{-2}	MPa^{-1}
a^k_3	1.36×10^{-2}	7.56×10^{5}	4.44×10^{-2}	1.07×10^{6}	
a^k_4	9.44×10^{-3}	4.55×10^{-3}	2.3×10^{-2}	9.65×10^{-3}	MPa^{-1}
Q^k_1	552	85.6	552	85.6	kJ mol^{-1}
Q^k_2	131	-82	131	-82	kJ mol^{-1}

$$\varepsilon_i = a_1^k \exp\left[a_2^k \sigma - \frac{Q_1^k}{TR} \right]$$

$$\beta K = a_3 \exp\left[+ \frac{Q_2}{TR} - a_4 \sigma \right]$$

It has been shown that if same constants are used to compute the creep strain time plot of a <111> crystal the strain accumulation due to octahedral slip is marginal [5]. This is primarily because of the fact that the resolved shear stress on the slip system is low as Schimds' Factor itself is small. In fact this is the reason why <111> crystals are likely to exhibit the best creep resistance provided slip takes place on octahedral slip systems only. However, several tests on <111> crystals of SRR99 show that the creep rate is indeed much higher than that predicted on this assumption [6]. This is an indication that certain other slip systems are getting activated when <111> is the tensile axis. There is some evidence that cube slip can occur in Ni base superalloys [13-15]. Ghosh et. al. gives a detailed justification of this [6]. Assuming such a slip to be operative it is possible to estimate the model parameters a_1, a_2 etc. for cube slip form <111> crystals assuming that in this case the contribution from octahedral slip towards creep is negligible. The constants thus obtained are given in the Table 4.

Having established the characteristic constants for octahedral and

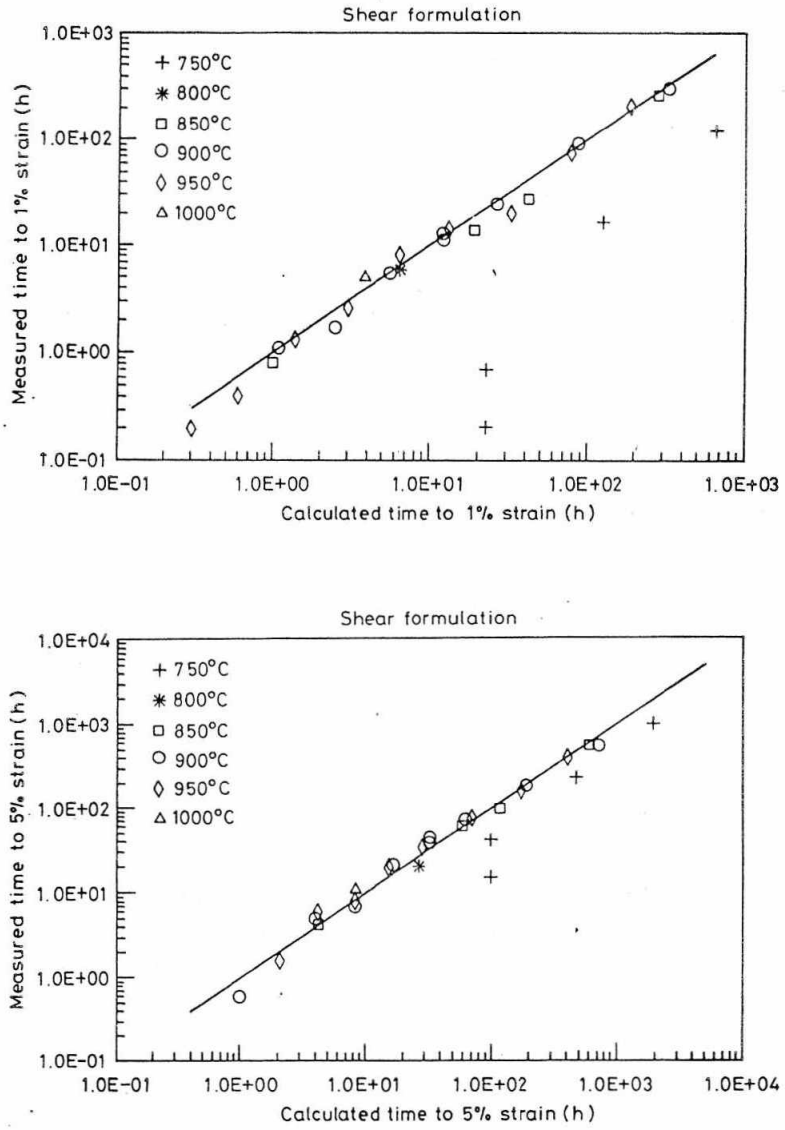

Fig. 3 : Comparison of measured times to various creep strains with the values calculated using the model parameters given in the Table 4(6) (a) time to 1% strain, (b) time to 5% sttrain

cube slip from an analysis of creep data for orientation where only one type of deformation dominates, it is possible to compute creep strains and the associated crystal rotation for crystals having arbitrary orientations where both types of slip can occur. The procedure assumes that the strains from the two deformation modes are additive.

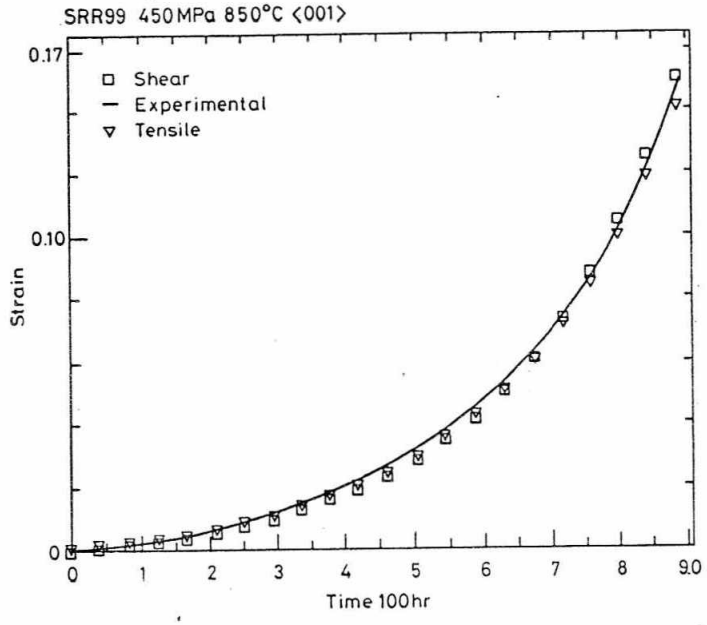

Fig. 4 : Comparison of the fits of the tensile and shear formulations to a typical experimental creep curve for <001> tensile orientation at 450 MPa/850°C (6)

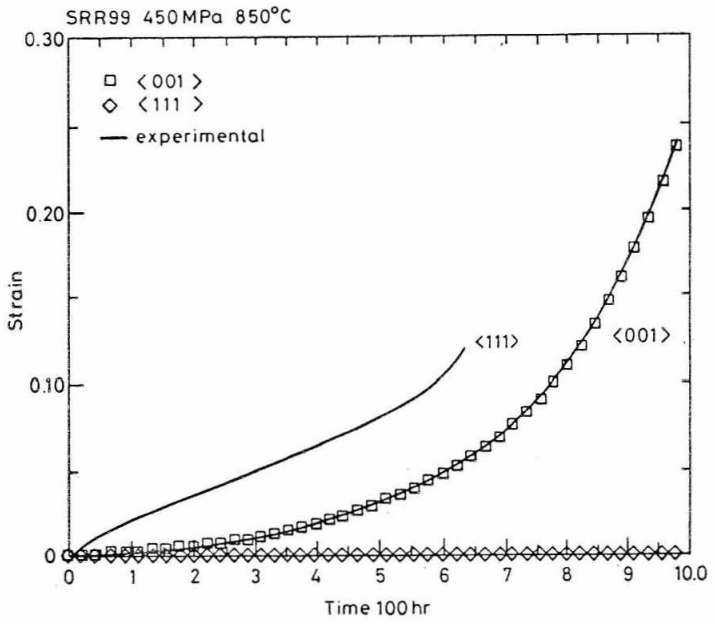

Fig. 5 : Comparison of predicted and experimental creep curves for <001> and <111> crystals of SRR99 tested at 450 MPa/850°C. Calculation is based on the assumption that only {111} <101> glide occurs (6).

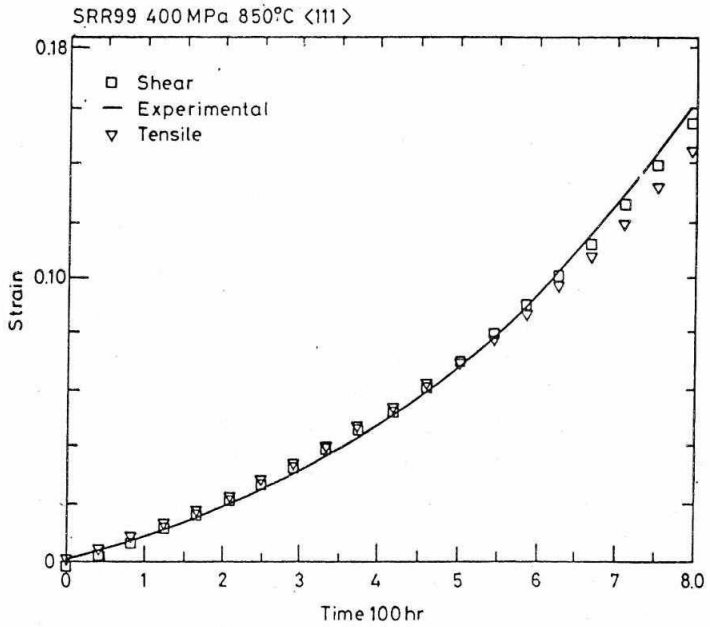

Fig. 6 : Same as Fig. 4 but for <111> tensile orientation tested at 400 MPa/850°C (6)

ANALYSIS OF CREEP

A fairly large creep database on <001> crystals of SRR99 was analysed by the approach described above. Fig. 3 gives comparison of predictions with experimental data. The predicted plots are obtained by numerical integration of equation sets (5) and (15) in the cases of tensile and shear formulations respectively. This was accomplished on an IBM PC using a modified Runge-Kutta method with adaptive step size control. The predictions based on shear formulation are as quite consistent with the experimental data over a wide range of temperature. Discripancy at lower temperature e.g., 750°C is due to the fact that here the effect of primary creep is significant whereas its effect in our present formulation has been neglected. At a temperature approaching 1050°C rafting is known to take place in Ni base superalloys, therefore it is quite natural to expect that a model based on strain softening mechanism will not be applicable in this regime. Fig. 4 gives a typical prediction of creep strain time curve for <001> crystal with experimental plot as well as prediction based on tensile formulation superimposed on the same. The excellent match is a clear indication

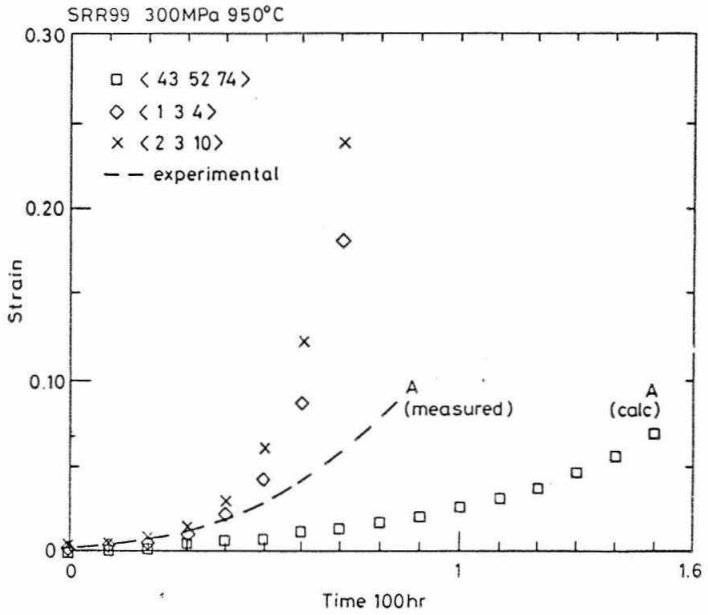

Fig 7 : Predicted creep curves for crystals having complex tensile axis axis, calculated on the assumption that glide occurs simultaneously on octahedral and cube slip systems (6).

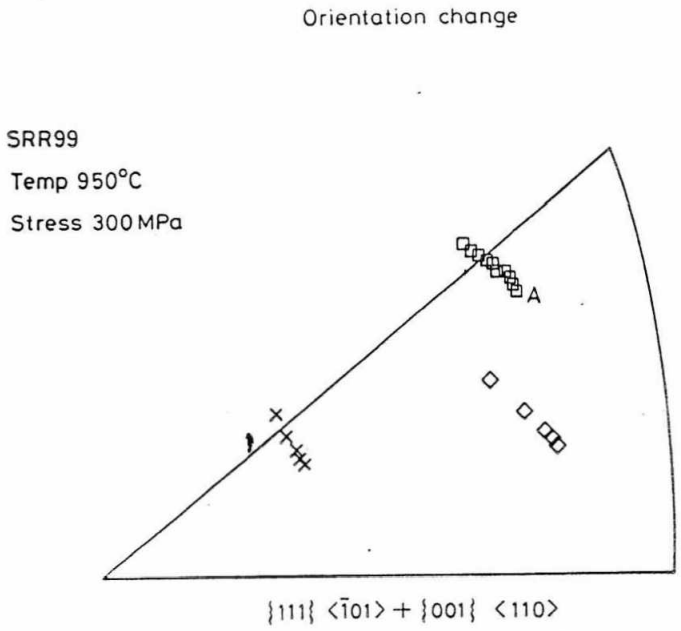

Fig. 8 : Expected rotations of the tensile axes for the cases included Fig. 7.

that shear formulation based on octahedral slip is capable of simulating the creep of single crystal.

Fig. 5 on the other hand gives a comparison of the measured creep curves of <001> and <111> crystals with those computed on the basis that slip takes place only on {111} <101> slip systems. This inicates that for <111> crystal contribution of octahedral slip towards creep is only marginal, though the experimental data show significant creep strain accumulation. This is possible only if certain other glides are operative. Cube slip is a possible alternative. Assuming that creep takes place by such glide in <111> oriented crystals it is thus possible to estimate the model parameters representing cube slip. Unlike <001> crystals creep database on <111> crystals of SRR99 is very limited. Therefore it is difficult to obtain a reliable estimate of material con-

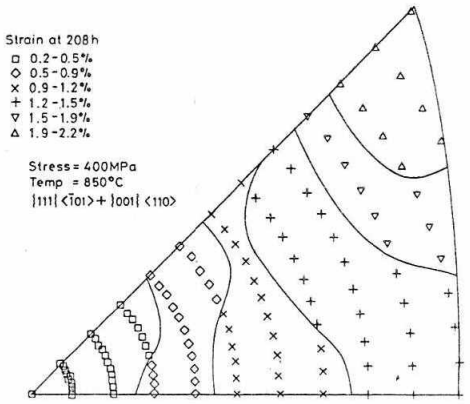

Fig 14(a)

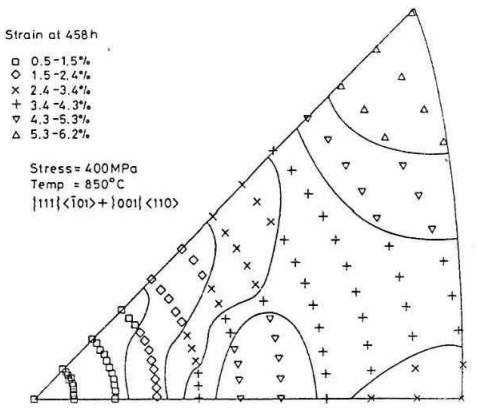

Fig. 9 : Calculated creep performance map for SRR99 displayed as contours in the unit stereographic triangle (a) Creep Strain after 208 h, (b) times to reach 10% strain (6)

stants for cube slip. However an approximate estimate of these on the basis of available data is given in the Table 4. Fig. 6 gives a typical creep curve for <111> oriented SRR99 single crystal simulated on the basis of shear along {100} <001> as well as tensile formulation. Both of these describe the experimental data reasonably well. The small difference in the predictions between shear and tensile formulation is a result of numerical computation and is insignificant when compared with scatter associated with creep performance.

SIMULATION OF CREEP FOR ARBITRARY ORIENTATION

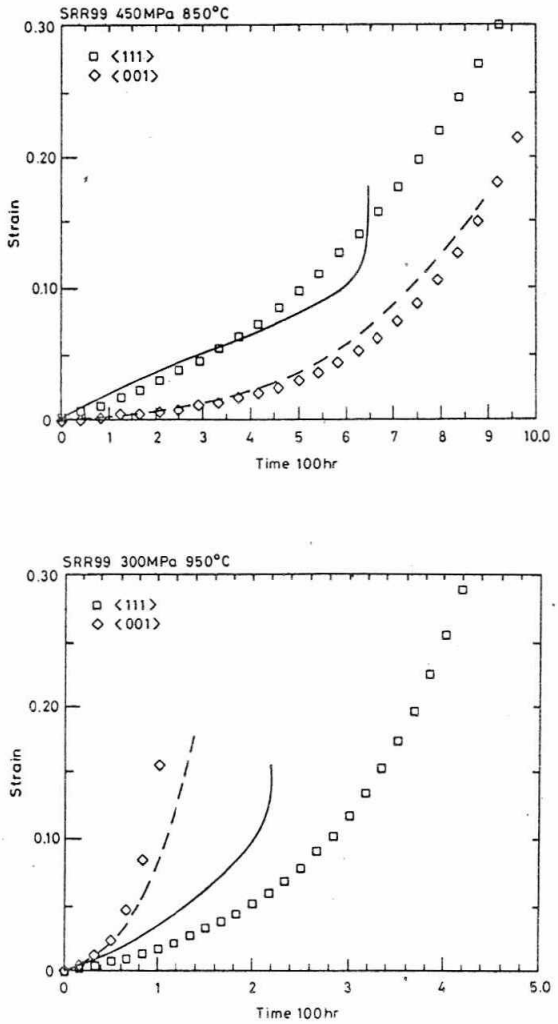

Fig.10 : Calculated and experimental creep curves for <001> and <111> crystals under two different conditions (a) 450 MPa 850°C, (b) 300 MPa 950°C

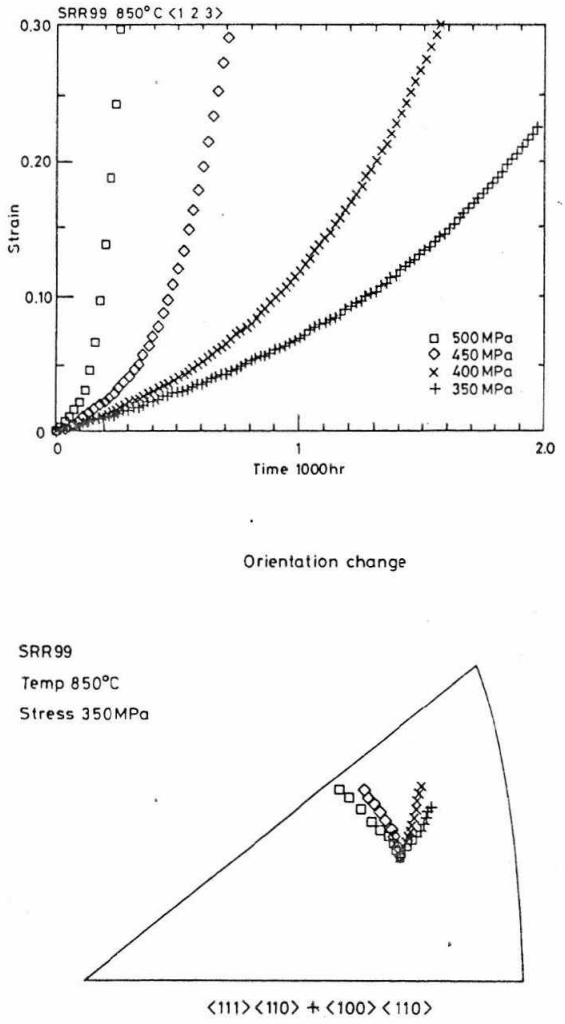

Fig.11 : Calculated creep performance for SRR99 with tensile axis <123> at 850°C and various stresses (a) creep curves, (b) crystal rotations (6)

Having established the material constants for shear creep on both {011} <110> and {111} <101> it is now possible to generate the creep curve for any arbitrary orientation where both types of glide operate.

Fig. 7 gives typical predictions of creep curves of crystals having complex initial orientations. In such case the tensile axis of the crystal rotates as a function of time. Fig. 8 depicts the expected rotation. This results from the activation of many slip vectors of two general families of slip systems and is quite different from that generally quoted as arising from the single slip vector. Experimental data for such complex

rotations are rare. Creep-curve for a given orientation A has been included in Fig. 7 for comparison.

Creep performance for a given stress and temperature has been estimated for initial orientations of crystal spread all over the unit stereographic triangle (Fig. 2) by changing the angular coordinates in steps of 5°. The anisotropy of its creep behaviour can then be displayed as contours of either time to achive specific strain or the strains at specific times as shown in the Fig. 9. This reveals that crystals near <001> have the best creep resistance at 850°C/400 MPA. However the kinetics of viscous glide on octahederal and cube slip system may have different stress and temperature dependence. Therefore it is expected that the nature of anisotropy of creep performance may change with initial stress and temperature.

This has been shown in Fig. 10 giving a comparison of the experimental and the simulated creep curve of <100> and <111> crystals under two different conditions of stress and temperature. This shows under one condition <001> crystal is stronger whereas under another <111> has better creep performance. This study also reveals that rotations can be extremely sensitive to the stress and temperature. Fig. 11b shows the changes in orientations associated with combined octahedral and cube glide at different stresses for the initial orientation <123> at 850°C. The corresponding creep curves have been presented in Fig. 11a. The change in the rotation is a result of changing contribution of cube slip towards total deformation with increasing stress.

DISCUSSION

The approach described in this work gives a new method of analysing anisotropy of creep behaviour of single crystals based on the mechanism of deformation. This has helped to explain some of the important features of creep deformation in SRR99 a Ni base superalloy. In order to explain its creep behaviour it was necessary to consider the contribution of two kinds of viscous glides viz. octahedral and cube glides. Though it is possible to obtain a fairly good estimate of the material constants necessary to model the kinetics of octahedral glide from a fairly large data base on <001> oriented crystals it is not possible to estimate these constants with same level of reliability for cube glide because of a very limited database on <111> crystals. With the availability of a large database on <111> crystals some of the predictions presented here may change considerably. The calculations

presented here should therefore be taken as indications of the type of information that could be obtained from such modelling.

It is evident that this type of modelling apart from predicting life gives a host of important information on the creep deformation of single crystals. The crystal rotation being quite sensitive to the type of viscous glide taking place, its measurement could be used to indentify the contribution of different types viscous glides. Crystals having symmetric orientation such as <001>, <111> and <011> do not undergo any rotation. Therefore these are the ideal cyrstals to characterize the kinetics of viscous glide. Thus the major steps involved in the complete charaterisation of the anisotropic behaviour of single crystal superalloy to allow reliable life prediction can be summarized as follows:

i) Perform creep tests on <001>, <011> and <111> oriented crystals to collect fairly large database over a range of stress and temperature.

ii) Estimate the material constants describing the octahedral and cubic glides.

iii) Simulate creep curves for a selected complex orientations and predict the expected rotation which could be verified by back scatter electron/X-ray diffraction patterns.

iv) Generate creep curves for crystals having all possible initial orientations to construct creep performance contours.

ACKNOWLEDGEMENTS

The author thanks Prof. M. Mclean for his guidance and encouragement during various stages of this work.

REFERENCES

[1] D.N. Duhl in *Superalloys II* (Edited by C.T. Sims et. al.), Wiley, New York, 1987.

[2] R.A. Mackey, R.L. Dreshfield and R.D. Maier, *Proc. of 4th Intl Symp. on Superalloys* (Edited by J.K. Tien et. al.), Metals Park, Ohio, ASM, 1980.

[3] D.M. Shah and D.N. Duhl, *Proc. of 5th Int. Symp. on Superalloys* (Edited by M. Gell et. al.), The Metallurgical Society of AIME, Warrendale, Pennsylvania, 1984.

[4] P. Caron, Y. Ohta, Y.G. Nakagawa and T. Khan, *Proc. of 6th Int. Symp. on Superalloys* (Edited by D.N. Duhl et. al.), The Metallurgical Society

of AIME, Warrendale, Pennsylvania, 1984.

[5] R.N. Ghosh and M. McLean, *Scripta Met.*, 23, 1989, pp1301.

[6] R.N. Ghosh and R.V. Curtis and M. McLean, *Acta Metall., Mater*, 38, 1990, pp1977.

[7] B.F. Dyson and M. McLean, *Acta Metall.*, 31, 1983, pp17.

[8] J.C, Ion, A. Barbosa, M.F. Ashby, B.F. Dyson and M. McLean, *NPL Report DMA A* 115, 1986.

[9] B.F. Dyson, Rev., *Phys. Appl.* 23, 1988, pp605.

[10] A. Kelly and Groves, Crysal and Crystal defects, Longman, London, 1970.

[11] M. Maldini and V. Lupinc, *Scripta Metall,* 22, 1988, pp1737.

[12] R.V. Curtis, P. Quested and M. McLean; unpublished work.

[13] B.H. Kear and B.J. Picarcey, *Trans. AIME,* 239, 1967, pp1209.

[14] V. Paidar, and D.P. Pope and V. Vitek, *Acta Metall,* 32, 1982, pp435.

[15] Y.Q. Sun and P.M. Hazzeldine, *Phil Mag.* A58, 1988, pp603.